CONTROLLED BUBBLE NUCLEATION IN GAS-LIQUID-SOLID CATALYTIC MICROSYSTEMS FOR ENHANCED MASS TRANSPORT

Renée M. Ripken[1], Jeffery A. Wood[1], Stefan Schlautmann[1], Axel Guenther[2], Johannes G.E. Gardeniers[1] and Séverine Le Gac[1]

[1]University of Twente, The Netherlands and
[2]University of Toronto, Canada

ABSTRACT

To obtain insight into transport phenomena in gas/liquid/solid catalytic microsystems, a theoretical model was developed to study heat and mass transfer at the microscale in such multiphase systems. In particular, systems were investigated in which the gaseous products nucleate and grow as microbubbles on the catalytic surface, whereas the reactants are dissolved in a liquid phase. A microfluidic platform providing spatial control on the bubble nucleation was designed and fabricated and applied to experimentally study the influence of bubbles on transport phenomena. The observations were compared with our theoretical model.

KEYWORDS: multiphase systems, catalysis, microfluidics, heat and mass transport

INTRODUCTION

The majority of industrial catalytic processes are heterogeneous; catalysts are solid while the reactants and products are in the gas and/or liquid phase. In some catalytic reactions, such as the reforming of alcohols and sugars, reactants are dissolved in liquid and products are formed as gases (*i.e.* H_2, CO and CO_2). Upon formation of gaseous products, bubbles nucleate and grow on the catalytic surface, resulting in a multiphase system where the interplay between different transport phenomena is relatively complex. Although the gas bubbles block the catalytic surface for further reaction, the convection in the channel is locally increased due to the slip boundary condition on the gas/liquid interface and could therefore positively influence the mass transport.

EXPERIMENTAL

To understand these systems, numerical simulations were carried out in COMSOL Multiphysics 5.2a. A 2D microreactor model was considered, with a 250-µm deep channel etched in silicon, and covered with glass (Figure 1A). A 10-µm thick TiO_2-layer at the bottom of this channel acted as the catalyst support layer. The system was heated from the silicon side and heat dissipated into air through the glass lid, while the rest of the system was considered thermally insulated. A no-slip boundary condition was assumed on both the channel wall and catalytic surface, and the bubble was treated as a perfect slip wall.

Next, a high-pressure and high-temperature set-up was developed to validate the numerical model (Figures 1B and 1C). The microfluidic device consists of a glass-silicon-glass stack, with a meandering channel (525 µm-deep and 500 µm -wide) etched through the central silicon layer. On the bottom glass layer a 65-nm thick ITO layer with Pt-contacts was deposited. The

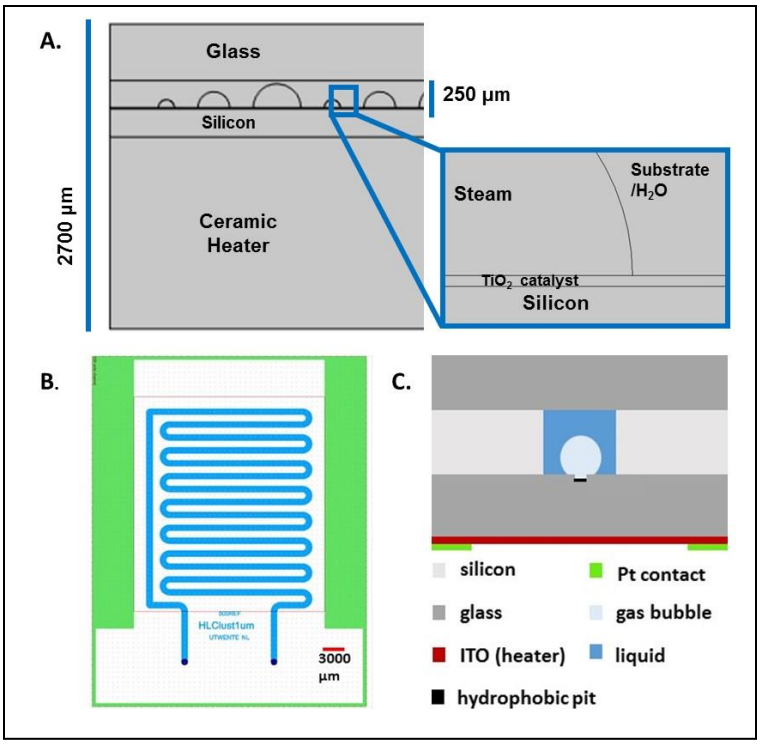

Figure 1: Design of the microfluidic device as used in the simulations (A) and for experiments (B and C); B. Top view, with in light blue the fluidic channel, and Pt-contacts in green; C. cross-section of the device (not to scale).

bottom glass layer comprises superhydrophobic (contact angle greater than 150^0) micropits (either 2 or 4 µm in diameter, aspect ratio 1:1), acting as preferential nucleation sites for the bubbles. To promote bubble coalescence and shorten the bubble departure time from the catalytic surface, micropits were clustered and their density varied. The microfluidic device was placed in a customized PEEK holder containing two optical windows, so that the assembly was completely transparent, facilitating microscopic imaging. A power supply was connected to pushpins touching the Pt contact. A K-type thermocouple was taped to the glass top layer to monitor the temperature during the experiments. As the microfluidic device did not contain any catalyst, bubbles were generated either through boiling of pure MilliQ water or CO_2 outgassing. In both cases, the device was heated at atmospheric pressure until gas formation was observed, and operated either with a flow rate of 10 µL.min^{-1} or without flow.

RESULTS AND DISCUSSION

The numerical simulations focused on the external mass transfer limitations, and included reaction kinetics. By varying the size of the bubbles and the distance between them, local higher fluid velocities were found in the microchannel. Similarly, mass transfer of the reactants and products, respectively to and from the catalytic layer was locally enhanced. However, the heat transfer was negatively affected, since gas bubbles act as an insulating layer, increasing the thermal entrance length compared to a system without bubbles (Figure 2). Consequently, in this system highly endothermic reactions would require a longer residence time to reach similar conversion as in a system without bubbles on the surface.

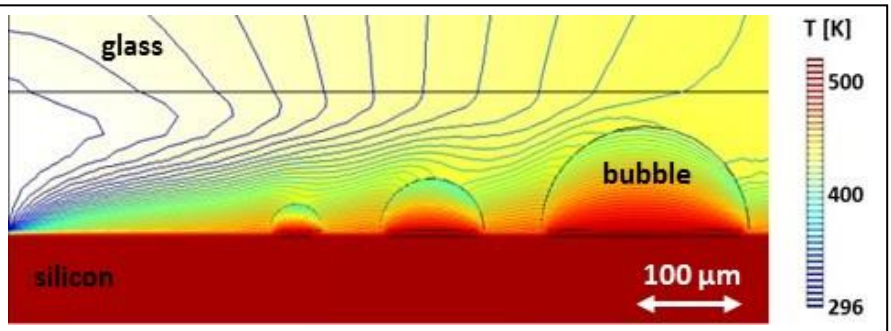

Figure 2: Temperature profile at the entrance of a microfluidic channel in which bubbles are growing at the catalytic surface. Heat is applied from the bottom of the channel, and is transported through the silicon. The bubbles hinder heat transfer to the fluid as a result of their insulating properties.

To control the transport phenomena experimentally, a microfluidic device was designed in which both the location and the size of bubble can be controlled. First, several layers of the microfluidic device were tested individually. Experiments in CO_2-supersaturated water with a glass layer containing the micropits confirmed that the micocavities were indeed active nucleation spots (Figures 3A & B). Thermal imaging using an IR camera demonstrated uniform heating of the microfluidic device (Figure 3C).

The current, power and temperature as a function of the applied voltage were characterized for the complete microfluidic device placed in its dedicated chip holder. From this data it was found that the resistance of the assembly is in the range of 60 to 85 Ohm. Although all the devices originated from the same wafer, these slight differences are likely to be caused by the fabrication processes, for example, due to the non-uniformity of the ITO deposition process and resulting variations in thickness.

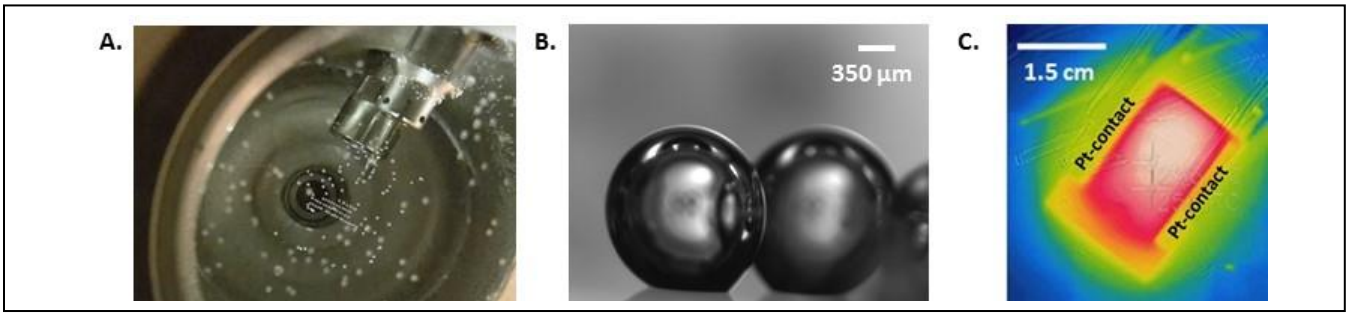

Figure 3: Bubble nucleation in a supersaturated CO_2/water mixture on the glass layer containing the hydrophobic pits only, observed from the top (A) and side (B). The bubbles are generated along the meandering pattern formed by the hydrophobic pits etched in the glass substrate. C. ITO heater, thermal image. The red color between the contacts indicate a homogeneous temperature field.

Vapor bubbles were created in the closed microchannels by boiling pure MilliQ water. In the reference design without pits, explosive boiling occurred at 115 ^{0}C, higher than the expected 100 ^{0}C at atmospheric pressure. This is indicative of superheating, which is consistent with this type of boiling mechanism. In devices with active micropits, however, nucleate boiling was observed, as the energy barrier to create a bubble is lowered by the presence of the cavities. In these devices, the first vapor bubbles formed at 85 ^{0}C (Figure 4).

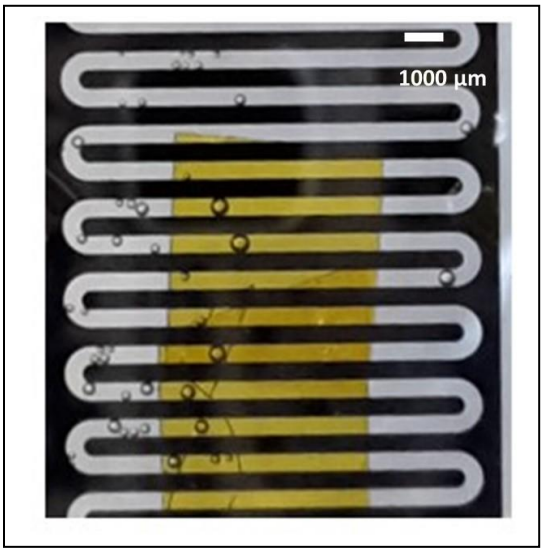

Figure 4: Vapor bubbles forming at the micropits at the bottom of the closed microchannel. Nucleate boiling occurred at 85 ^{0}C.

Boiling is a too violent process to properly control the bubble size. More gentle is the formation of gas bubbles out of a supersaturated CO_2/H_2O solution by slowly increasing the temperature; the CO_2 solubility decreases when increasing the temperature, resulting in outgassing, bubble nucleation and bubble growth. Typically, the first bubbles were observed at 45 ^{0}C, and continued to grow as long as heat was applied to the device.

For mass transport, the system is easier to study at a steady-state, *i.e.* with static bubbles. First the microchannel was completely filled with the CO_2/H_2O solution at 10 µL/min. Outgassing was induced by shortly heating the device without liquid flow. By switching off the heat as soon as the first bubbles appeared, the bubbles could be kept smaller than the channel diameter. Therefore, the liquid could still flow freely past the gas bubbles, which prevented a local pressure build-up, and a steady pressure drop along the channel was maintained.

The stability of these microbubbles was characterized by increasing the liquid flow rate. Surprisingly, the bubbles remained fixed at their pits at least up to a flow rate of 250 µL/min, likely because the bubbles were strongly pinned to their microcavities. The bubbles could be removed, however, by large gas slugs, which formed when a bubble was growing to a size larger than the microchannel diameter. These results demonstrate that the bubbles are pinned beyond the micropit radius.

Repeating the nucleation experiments revealed that micropit deactivation was observed after on average 20 cycles of nucleation (Figure 5A - 5E). The exact deactivation mechanism is unclear, but it is likely related to the micropit filling with water: once the gas nucleus is removed, no new bubbles can grow from that particular cavity. Filling of the micropits with water could occur due to several reasons, such as applying a too high hydrodynamic pressure, removal of the fluorocarbon layer rendering the micropit superhydrophobic, and formation of a small microjet after a bubble has collapsed.[1] The micropits could be reactivated by removing all the liquid (Figure 5E). The microfluidic device was cleared of the liquid and subsequently heated at 175 ^{0}C for 45 minutes. Next, the microchannel was carefully refilled with liquid at a flow rate of 10 µL/min, to ensure the hydrodynamic pressure was low enough so that the liquid was not forced in the micropits again. Boiling experiments were then resumed, showing that the micropits can be temporarily re-activated for around 5 cycles.

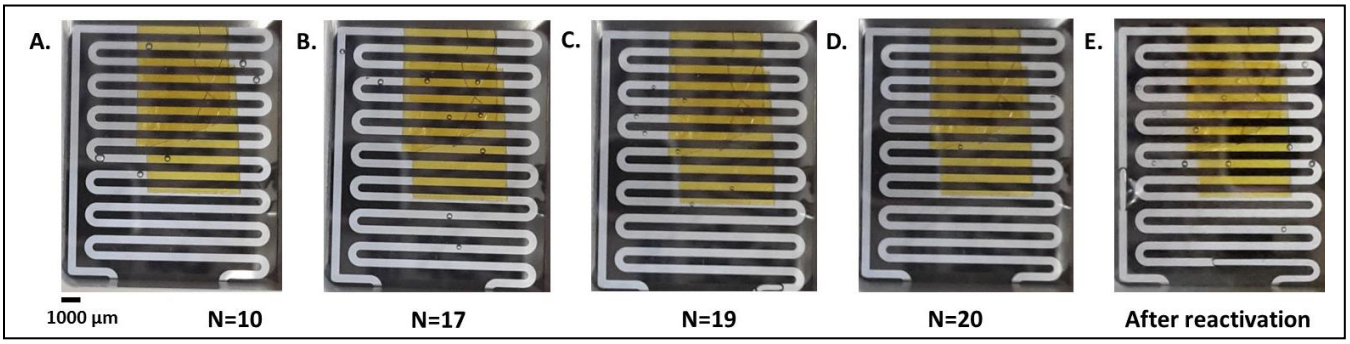

Figure 5: Micropit deactivation and reactivation, with N being the number of cycles. After 20 cycles (D), almost no nucleation was observed. The micropits were reactivated by heating for 45 minutes at 175 ^{0}C (E).

Once relatively good control over the bubble nucleation and size was obtained, the bubble patterns were studied as a function of the pit design. Although microcavities were located continuously along the channel, bubbles almost never formed in close proximity to each other, which could be explained by the local pressure increase associated with bubble nucleation: when a bubble has to nucleate close to another bubble, it has to overcome a slightly higher pressure. The observation that a bubble in close proximity to another, already growing bubble, nucleated at a later time than the first bubble, seems to support this hypothesis.

Furthermore, it was not possible to distinguish between different bubble patterns, growth rates or sizes across the different designs. For catalysis, the designs comprising micropit clusters were of special interest, as bubbles were expected to coalesce, to depart faster and therefore vacate the catalytic surface faster for further reaction. Although, no bubble coalescence was observed during the experiments, it could be that it occurred at a shorter timescale than the camera could record.

CONCLUSION

Transport phenomena in gas/liquid/solid catalytic microsystems are fairly complex. Although the gas bubbles block the catalytic surface for further reaction, it was shown by numerical simulations using COMSOL Multiphysics that the bubbles can also be exploited to enhance the mass transport. Next, a microfluidic device containing superhydrophobic micropits to control the location of the bubble formation was designed and fabricated. By accurate heat supply to the system, it was possible to prevent bubbles from growing larger than the channel diameter. As a result, the bubbles did not block the channel and the liquid could still freely flow passed the bubbles, thereby preventing local pressure build-up. These gas bubbles were stable at least up to a flow rate of 250 $\mu L.min^{-1}$. In the future, this microfluidic set-up will be further developed to optimize the transport phenomena in catalytic three-phase reactions.

ACKNOWLEDGEMENTS

This work was supported by the Netherlands Center for Multiscale Catalytic Energy Conversion (MCEC), an NWO Gravitation programme funded by the Ministry of Education, Culture and Science of the government of the Netherlands.

The author would like to thanks Álvaro Moreno Soto, University of Twente, The Netherlands for his contribution to the CO_2 outgassing experiments with the open channel configuration.

REFERENCES

[1] B. M. Borkent, S. Gekle, A. Prosperetti and D. Lohse, "Nucleation threshold and deactivation mechanisms of nanoscopic cavitation nuclei," *Phys.Fluids*, 21, 102003-102003-9, 2009.

CONTACT

* R.M. Ripken; phone: +31 534892019; r.m.ripken@utwente.nl